HHS Public Access

Author manuscript

Stem Cells. Author manuscript; available in PMC 2016 April 01.

Published in final edited form as:

Stem Cells. 2015 April ; 33(4): 1241–1253. doi:10.1002/stem.1965.

Pulsed focused ultrasound pretreatment improves mesenchymal stem cell efficacy in preventing and rescuing established acute kidney injury in mice

Scott R. Burks, PhD[1,2,*], **Ben A. Nguyen, MS**[1], **Pamela A. Tebebi, MS**[1,3], **Saejeong J. Kim, PhD**[1], **Michele N. Bresler, BS**[1], **Ali Ziadloo, BS**[1], **Jonathan M. Street, PhD**[4], **Peter S. T. Yuen, PhD**[4], **Robert A. Star, MD**[4], and **Joseph A. Frank, MD**[1,5]

[1]Frank Laboratory, Radiology and Imaging Sciences, Clinical Center, National Institutes of Health, Bethesda, MD 20892

[2]Imaging Sciences Training Program, Clinical Center and National Institute of Biomedical Imaging and Bioengineering, National Institutes of Health, Bethesda, MD 20892

[3]Department of Biomedical Engineering, The Catholic University of America, Washington, DC 20064

[4]Renal Diagnostics and Therapeutics Unit, Kidney Diseases Branch, National Institute of Diabetes and Digestive and Kidney Diseases, Bethesda, MD 20892

[5]Intramural Research Program, National Institute of Biomedical Imaging and Bioengineering, Bethesda, MD 20892

Abstract

Animal studies have shown that mesenchymal stem cell (MSC) infusions improve acute kidney injury (AKI) outcomes when administered early after ischemic/reperfusion injury or within 24hr after cisplatin administration. These findings have spurred several human clinical trials to prevent AKI. However, no specific therapy effectively treats clinically obvious AKI or rescues renal function once advanced injury is established. We investigated if noninvasive image-guided pulsed focused ultrasound (pFUS) could alter the kidney microenvironment to enhance homing of subsequently infused MSC. To examine the efficacy of pFUS-enhanced cell homing in disease, we targeted pFUS to kidneys to enhance MSC homing after cisplatin-induced AKI. We found that pFUS enhanced MSC homing at 1 day post-cisplatin, prior to renal functional deficits, and that enhanced homing improved outcomes of renal function, tubular cell death, and regeneration at 5 days post-cisplatin compared to MSC alone. We then investigated whether pFUS+MSC therapy could rescue established AKI. MSC alone at 3 days post-cisplatin, after renal functional deficits were obvious, significantly improved 7-day survival of animals. Survival was further improved using pFUS+MSC. MSC, alone or with pFUS, changed kidney macrophage phenotypes from M1 to M2. This study shows pFUS is a neoadjuvant approach to improve MSC homing to diseased

[*]To whom correspondence should be addressed: Scott R. Burks, Ph.D., 10 Center Dr., Rm. B1N256, Bethesda, MD 20892, Ph: 301-594-2368, Fax: 301-402-3216, scott.burks@nih.gov.

DISCLOSURES

Authors have no disclosures.

organs. pFUS with MSC better prevents AKI than MSC alone and allows rescue therapy in established AKI, which currently has no meaningful therapeutic options.

INTRODUCTION

Acute kidney injury (AKI) occurs commonly in hospitalized patients and can have mortality rates up to 50% when associated with co-morbid non-renal illness or surgical complications [1–4]. Most current clinical trials are designed to prevent deterioration of renal function, as older clinical studies suggested that rescuing established AKI would be difficult [5–7]. Intravenous infusion of bone marrow stromal cells, also known as mesenchymal stem cells (MSC), have been tested in animals to prevent AKI before the disease can be clinically diagnosed. MSCs reduce subsequent renal functional deficits, tubular necrosis and apoptosis, and promote tubular regeneration, likely through paracrine or endocrine effects rather than engraftment [8–11]. The exact therapeutic mechanisms of MSC in AKI are still poorly understood. After systemic infusion, MSCs become primarily entrapped in the lung [12], while a small proportion of cells can home to other organs (e.g., spleen or liver) and sites of inflammation. Some studies suggest that MSCs can act from distant organ sites (e.g. lung or spleen) to modulate inflammation and promote regeneration in the kidney [8]. However, numerous other studies have shown that MSC residing in the kidney tissue following infusion through the renal artery are capable of improving AKI [13, 14]. Because of the promising pre-clinical data, MSCs are being tested in clinical trials designed to prevent the occurrence of AKI (NCT01602328, NCT00733876; www.clinicaltrials.gov).

Direct injection of MSCs into feeding arteries or organs is difficult, cellular therapies would ideally be administered by intravenous (i.v.) infusion. Circulating cells can home to pathological loci [15, 16]—a process that is inefficient [17] and difficult to control. Several strategies to gain spatio-temporal control over cell homing have been developed [18], but are invasive, imprecise, or not readily translatable to the clinic. Image guided focused ultrasound is FDA-approved for thermal ablation of uterine fibroids [19]. Pulsed focused US (pFUS) exposures allow cooling between individual sonications [20] so that mechanical interactions between ultrasound and tissue predominate. We previously demonstrated in healthy murine skeletal muscle and kidneys that pFUS alone was benign and presumably through mechanotransduction, elicited transient local increases of chemoattractants (cytokines, chemokines, trophic factors, and cell adhesion molecules) in sonicated tissue that is termed a “molecular zip code” [21, 22]. Coupling i.v. infusions of unmodified human MSCs or endothelial precursor cells with pFUS enhanced margination and active transmigration of cells into healthy pFUS-treated skeletal muscle or kidneys (Figure 1A) [21, 23].

We previously studied pFUS and stem cell homing in healthy tissue; the utility of pFUS in injured tissue is unknown. Since AKI is responsive to both intravenous and intra-arterial MSC therapy, we explored the therapeutic effects of combining pFUS with MSC infusions in a mouse model of AKI. Cisplatin-induced AKI is characterized by widespread proximal convoluted tubular degeneration and necrosis in cortico-medullary regions, leading to renal dysfunction [24]. Peak loss of renal function occurs 3–5 days following cisplatin

administration with recovery by 7–10 days [25]. We hypothesized that pFUS could potentially generate enhanced homing permeability and retention (EHPR) of MSCs during AKI by altering the local molecular profiles to increase chemoattractant expression as we have previously observed in healthy kidney and skeletal muscle [21, 23]. We also examined whether pFUS enhanced MSC homing could confer additional therapeutic benefits during early AKI, compared to current systemically administered MSC therapies [10, 26, 27]. However, previously published MSC therapies for AKI were administered before functional deficits became obvious; hence, it is also unknown whether MSCs could rescue function or improve survival during established AKI. Thus, we explored the effects of delayed treatment with pFUS and MSCs or MSCs alone at 3 days post-cisplatin, during clinically obvious AKI.

MATERIALS AND METHODS

Animal studies

The Animal Care and Use Committee at our institution approved all animal procedures. AKI was induced in female C3H mice (Charles River Laboratories, Wilmington, MA) weighing 25–30g by i.p. injection of cisplatin at 15mg/kg (Cadilia Healthcare, Ahmedabad, India). Food and water were withheld from mice for 12h before cisplatin injection until after cisplatin injection. Treatment times for established AKI experiments (MSCs and/or pFUS on Day 3 post-cisplatin) were derived from the natural history of cisplatin-induced AKI in this mouse strain (Supplemental Figure 3). For each experiment (D1 or D3 treatment), mice were divided into 4 groups: AKI (cisplatin [Cis] only), Cis+MSC (no pFUS), Cis+pFUS+MSC, and Normal controls (sham treatments for cisplatin, pFUS, and MSC). For D1 treatment, cisplatin was injected on Day 0 and bilateral pFUS and/or MSC were administered on D1. On D4 post-cisplatin, mice were euthanized and kidneys were dissected for histology and serum was collected for BUN and SCr measurements. The D3 treatment used the same 4 groups of mice with the exception that treatment with bilateral pFUS and/or MSC infusions were delayed until D3 post-cisplatin. Plasma samples were collected on D4 and D6 post-cisplatin and surviving animals were euthanized on D7 post-cisplatin.

pFUS technique

pFUS was administered with a Sonoblate 500 (Focus Surgery, Indianapolis, IN) under ultrasound imaging guidance. [21] pFUS exposure parameters were: peak rarefaction amplitude, 8.9 MPa; pulse repetition frequency, 5 Hz; duty cycle, 5%; number of pulses per site, 100. Six raster points in a 2×3 pattern with an elemental spacing of 2 mm were used to treat kidneys. Kidneys were treated unilaterally for molecular analyses and quantification of MSC homing, where untreated contralateral kidneys were internal controls. Bilateral pFUS was performed in mice used to assess functional outcomes. Control groups received sham pFUS exposures (transducer power=0 W).

Culture, Characterization, and Injection of MSCs

Human MSCs (NIH Center for Bone Marrow Stromal Cell Transplantation) were culture-expanded in α-minimum essential medium (Life Technologies) with 20% fetal bovine serum (Gemini, Sacramento, CA), 0.29 mg/mL L-glutamine (Life Technologies), and 1%

penicillin/streptomycin (Life Technologies) at 37 °C under 5% CO_2 and 1% O_2. Early passage MSCs (<5) were used and were characterized for cell-surface markers by conventional flow cytometry protocols using an Accuri C6 flow cytometer (Supplemental Figure 1). [22] For i.v. infusions, MSCs were treated with TrypLE (Life Technologies) and resuspended at 10^7 cells/mL in Roswell Park Memorial Institute-1640 medium (Life Technologies) containing 1 U/mL Heparin (sodium salt) (Hospira). 10^6 MSC were i.v. injected in the lateral tail vein 3–4h post-pFUS. ~5 min before MSC injections, all groups were administered i.v. sodium nitroprusside (Hospira, Lake Forest, IL) at 1 mg/kg. [12, 21]

Detection of human MSC after injection

Mice were euthanized and perfused with 4% PFA 24h post-MSC injection. Tissue sections were visualized using fluorescence immunohistochemistry (fIHC) for human mitochondria. [21, 23] Human-mitochondria-positive cells were counted in 10 high-power fields-of-view (FOV) per kidney by confocal microscopy.

Analysis of chemoattractants

Four hours after pFUS, treated and contralateral kidneys were dissected and frozen in liquid N_2. Kidneys were homogenized in cell lysis buffer (Cell Signaling Technology, Beverly, MA) with protease inhibitors (Santa Cruz, Santa Cruz, CA). Total protein concentrations were determined by bicinchoninic acid (Thermo Scientific, Waltham, MA). Homogenates (2 mg of total protein/mL) were analyzed by multiplex ELISAs (23-plex and 9-plex mouse kits [catalog #s M60-009RDPD and MD0-00000EL, respectively] or the human 27-plex kit [catalog #M50-0KCAF0Y], BioRad, Hercules, CA) using a Bio-Plex 200 system (For list of measured cytokines, see Supplemental Tables 1 and 2). ICAM, VCAM, and SDF-1α were measured with single-plex ELISAs (RayBiotech, Norcross, GA) at concentrations of 0.5 mg/mL.

Renal function measurements

BUN and SCr were measured by spectrophotometry or high-pressure liquid chromatography (HPLC) described previously. [21, 28]

Histological and Immunohistochemical Analyses

Tissues were fixed for 24h in PFA, followed by equilibration in 30% sucrose. For fIHC, histological sections (10 μm) were boiled in citrate buffer (pH=6.0) for 10 min and blocked using SuperBlock (Scytek, Logan, UT) for 15 min. Primary antibodies (all from Abcam; Cambridge, MA) for human mitochondria (mouse, 4 μg/mL), Ki-67 (rabbit, 2.5 μg/mL), F4/80 (rat, 10 μg/mL), CD11c (mouse, 5 μg/mL), CD206 (hamster, 4 μg/mL), CD31 (rabbit, 4 μg/mL), CD11b (rabbit, 5 μg/mL), or pAKT (rabbit, 2 μg/mL) were incubated overnight at 4 °C. Species-appropriate AlexaFluor-conjugated secondary antibodies (488, 568, or 647 nm; all from Abcam) were incubated 2h at room temperature. Slides were coverslipped with a DAPI-containing mounting medium. Background controls for fIHC used isotypes from the primary-antibody-appropriate species. Apoptosis was detected using a TUNEL assay (Life Technologies) [22]. Background controls for apoptosis assays omitted the TUNEL enzyme.

Microscopy and image analyses

Histology was visualized using a ScanScope CS (20× air objective, NA=0.75, Aperio Technologies, Vista, CA). fIHC was visualized on a laser scanning confocal microscope (Zeiss 710) using Plan-Apochromat objectives (20× air, NA=0.8; 63× oil-immersion, NA=1.4). Illumination was provided by argon-ion (Lasos, Jena, Germany), diode, and diode-pumped solid-state lasers (Roithner Lasertechnik, Vienna, Austria). Identical laser/microscope settings were used for quantitative imaging. For fIHC, mean pixel intensity and SD were determined for background controls with each stain. Fluorescence >2 SD above the mean background was considered positive. For quantitative analysis of F4/80, CD11c, and CD206, fluorescence-positive pixels were counted in 10 fields of view (FOV) per slide. The numbers of CD11c- and CD206-positive pixels in each FOV were normalized to the number of F4/80-positive pixels in that FOV. Non-macrophage CD11c was counted after images were masked for F4/80 signal intensity. Other fluorescence-positive features were manually counted in 10 FOV per slide. Light microscopy (H&E) surveyed 10 FOV per slide. All images were analyzed under blinded conditions.

Statistical Analyses

All data are presented as the mean ± SD. *T*-tests were used for pairwise comparisons and ANOVA with Bonferroni post-hoc analyses for multiple comparisons. Kaplan-Meier curves were analyzed by log-rank tests. All statistical tests were two-sided and $p<0.05$ was considered statistically significant. Data analyses and presentation were performed using Prism6 (GraphPad, La Jolla, CA).

RESULTS

Effect of pFUS on cellular homing

AKI was induced in mice by cisplatin on Day 0 (D0) and treatment schedules are shown (Figures 1B, 2B, 3A, 4A, 6A, and 7A). To assess whether pFUS increased MSC homing to kidneys at different time points during AKI, unilateral pFUS was administered on either D1 (early AKI) or D4 (late AKI), followed by 10^6 i.v. human MSC 4h post-pFUS. MSC preferentially homed to pFUS-treated kidneys compared to contralateral control kidneys at each time point, as detected by immunofluorescence for human mitochondria (Figures 1C and D). pFUS increased MSC homing by ~2-fold on either day compared to untreated kidneys (ANOVA, $p<0.05$). Significantly greater MSC homing was also observed to untreated kidneys (no pFUS) on D4 compared to untreated kidneys on D1 (ANOVA, $p<0.05$).

Effect of pFUS on the kidney

To understand pathological changes in the local tissue milieu during AKI, tissue chemoattractants and pro-/anti-inflammatory cues were measured over time during AKI alone (i.e., no pFUS, no MSC) and many were found to be at sub-physiological levels on D1, then elevated by D3, and sustained through D5 (Figure 2A). We then investigated how unilateral kidney pFUS on either D1 or D4 would alter the tissue environment of kidneys during AKI. Tissue levels of many known chemoattractants were significantly altered

compared to untreated contralateral kidneys 4 h after pFUS administered on either day (*t*-test for paired comparisons or ANOVA for multiple comparisons; $p<0.05$) (Figure 2C and D). This time point is close to the time when MSCs would be i.v. injected and when pFUS elevates several chemoattractants in normal kidney tissue [21]. pFUS on D1 increased tissue concentrations of vascular cell adhesion molecule (VCAM), intercellular adhesion molecule (ICAM), macrophage inflammatory protein (MIP)-1α, interferon (IFN)-γ, fibroblast growth factor (FGF), granulocyte colony-stimulating factor (G-CSF), and interleukins (IL)-1α, -1β, -2, -12p40, -12p70, and -18. pFUS also lowered levels of tumor necrosis factor (TNF)-α, macrophage inflammatory protein (MIP)-1β, macrophage colony-stimulating factor (M-CSF), granulocyte macrophage colony-stimulating factor (GM-CSF), and IL-4, -5, -15, and -17. pFUS given on D4 increased levels of VCAM, platelet-derived growth factor (PDGF), leukemia inhibitory factor (LIF), MIP-1β, MIP-2, INF-γ, M-CSF, G-CSF, and IL-1α, -3, -4, -5, -6, -8, -10, -12p40, -13, -15, -17, and -18. pFUS on D4 decreased vascular endothelial growth factor (VEGF). Stromal cell derived factor-1α (SDF-1α) increased during AKI, but was not altered by pFUS. These changes in the local tissue environment occurred without increased expression of heat shock protein (HSP) 70 in treated kidneys (Supplemental Figure 2).

Effects of pFUS alone

Since the effects of pFUS alone during AKI were unknown and many chemoattractants represent potential therapeutic targets in AKI [29, 30], we examined whether pFUS alone altered AKI progression. Bilateral kidney pFUS was performed on D1 post-cisplatin and animals were evaluated on D4. No differences in renal function (BUN/SCr), morphology, apoptosis, tubular Ki67 expression, or phosphorylated AKT (pAKT) were observed compared to animals receiving sham pFUS (*t*-test, $p>0.05$) (Figure 3).

Therapeutic efficacy on day 1 post-cisplatin

To examine the early therapeutic effects of pFUS coupled with MSCs, we employed a protocol similar to previous studies [10]. Cisplatin was administered on D0 and mice received either 10^6 MSCs i.v. alone or pFUS+MSC (10^6 i.v.), on D1, which precedes renal insufficiency (Supplemental Figure 3). Mice were euthanized on D4 and serum and kidneys were harvested. Consistent with previous studies, MSC alone reduced BUN by ~40%, apoptosis by ~40%, and necrosis by ~33% (Figure 4) compared to mice treated with cisplatin only (i.e., untreated) (ANOVA, $p<0.05$). In mice that received pFUS+MSC administered on D1, more human MSCs were detected in kidneys at D4 (Figure 4B) and the persistence of MSCs provided further protection against AKI compared to untreated mice by reducing BUN and SCr by ~65% and ~80%, respectively. Mice receiving pFUS+MSCs also showed significant improvements in BUN and SCr (ANOVA, $p<0.05$) compared to those receiving MSCs alone (Figure 4). Moreover, pFUS+MSC reduced apoptosis by ~60% and necrosis by ~80% compared to untreated mice (ANOVA, $p<0.05$). Only pFUS coupled with MSCs significantly increased tubular Ki67 and pAKT expression compared to untreated controls or mice that were infused with MSCs alone (Figures 4C and D).

Effect of late therapy

To determine the effect of MSC with or without pFUS during established AKI, treatment was administered at D3 post-cisplatin. Renal function, measured by BUN and SCr concentrations, is diminished by this time (Supplemental Figure 3) [31], and it was ideal to investigate whether MSCs can rescue renal function. Intravenous MSCs alone at D3 modestly, but significantly improved survival to D7 compared to untreated controls (log-rank test, p=0.0292) (Figure 5B). Enhancing MSC homing by pFUS further improved survival compared to MSC alone (log-rank test p=0.0247) and untreated controls (log-rank test, p<0.0001). Furthermore, a significant reduction in BUN was observed after pFUS and MSCs at D4 (24h post-treatment) that persisted through D6 (72h post-treatment) (ANOVA, p<0.05) (Figures 5C and D).

Effect of MSC and pFUS on immune cells, renal vasculature, and cytokines/growth factors

Changes in immune cell populations and vessel density are summarized in Figure 6. The phenotype of kidney macrophages shifted from M1 toward M2 after treatment with MSCs or pFUS+MSCs. Mouse macrophages (F4/80-positive) were characterized as M1 (CD11c expression) or M2 (CD206 expression). F4/80-positive macrophages in cisplatin-treated mice (no MSCs) showed significantly higher levels of CD11c expression and lower levels of CD206 expression (ANOVA p<0.05). After MSCs alone or pFUS+MSCs, CD11c expression decreased while CD206 expression increased on macrophages (ANOVA p<0.05). CD11b expressed by natural killer (NK) cells was significantly reduced by MSCs alone and further reduced by pFUS+MSCs (ANOVA p<0.05). CD11c that is expressed on F4/80$^-$ (non-macrophage) dendritic cells (DC) was not significantly reduced by MSCs alone, but was reduced by pFUS+MSC (ANOVA p<0.05). Vessel density, as assessed by CD31 staining of endothelial cells, was not significantly altered following treatment with MSC alone (ANOVA p>0.05), but was significantly increased following pFUS+MSC treatment compared to untreated mice (ANOVA p<0.05).

Treatment with pFUS and MSC altered levels of cytokines and growth factors in both the kidney and blood. Kidneys and serum from control AKI mice and animals treated with MSCs or pFUS+MSC were harvested and analyzed by multi-plexed ELISAs specifically for mouse or human protein expression (Figure 7). Since xeno-transplantation of human MSC was employed, factors produced by the MSCs and the host mouse tissue can be distinguished in both local kidney tissue and blood. Many human factors produced by MSCs were undetectable by ELISA in the serum or the kidney (data not shown); however, human IL-10 levels were significantly greater (ANOVA p<0.05) in the mouse kidney following pFUS+MSC treatment compared to either MSCs alone or control AKI mice (no MSC) (Figure 7B). Sampling the serum and kidney for mouse factors revealed significantly greater expression of mouse VEGF and decreased mouse TNFα (ANOVA p<0.05) in the kidney (Figure 7C). Furthermore, significantly greater mouse VEGF was also detected in the serum (ANOVA p<0.05) (Figure 7D).

DISCUSSION

The major findings of this study are as follows: 1) clinically tolerated doses of pFUS given during early or established AKI significantly increased renal MSC homing; 2) pFUS+MSC was more effective than MSC alone for early treatment of AKI; and 3) whereas late administration of MSCs improved survival, late pFUS+MSC further improved survival and renal function.

pFUS enhanced renal MSC homing

Successful MSC therapy may require transient localization of MSCs for 3–4 days post-infusion and strategies to improve homing are desperately needed [9]. After infused MSCs navigate the circulation, they can accumulate at pathological loci [32] by firm tethering to the vasculature cell adhesion molecules (CAMs), followed by transmigration into the parenchyma toward gradients of cytokines, chemokines, and trophic factors (CCTF) [15]. Homing of i.v. MSCs to many organs is inefficient and approaches to improve delivery to tissues focus on either genetic [33] or chemical modifications of cells [34], or stimulation of host tissue to promote recruitment [18], including using pFUS with microbubble ultrasound contrast agents [35–40]. However, such approaches are difficult to translate clinically and face regulatory difficulty because modified cell products or tissue damage following stimulation need to be carefully tested and monitored.

We previously characterized homing of i.v. MSC after pFUS to healthy skeletal muscle and kidneys [21–23]. pFUS alone did not damage tissue, and vessels remained impermeable to micron-sized bodies [20, 22], including red blood cells. pFUS created a transient “molecular zip-code” consisting of localized increased levels of CCTF, and CAMs (24–72h) [21–23] without HSP-70 elevation [23]. Therefore, pFUS is more likely to elicit local molecular responses through mechanotransduction, rather than tissue heating, and thus promote homing of circulating stem cells that was followed by cellular transmigration into the parenchyma. However, enhanced cell homing with pFUS had yet to be observed in diseased tissue, where microenvironmental changes from pFUS might be dampened because of ongoing acute inflammation. In our cisplatin-induced AKI model, pFUS alone increased CAMs and chemoattractants either before (D1) or during (D4) clinically detectable AKI, and significantly more MSCs were observed in peritubular spaces of pFUS-treated kidneys on either day. Following unilateral pFUS treatment, more MSCs homed to the contralateral non-pFUS-treated kidneys on D4 than D1, that could be due to more injury-induced chemoattractants on D4 compared to D1 (Figure 2A) [15]. Nevertheless, enhanced homing on either day was observed when MSCs were coupled with pFUS. Increased CAM in pFUS-treated kidneys could increase MSC localization and persistence compared to non-pFUS-treated kidneys. Of note, SDF-1α plays a significant role in MSC homing, especially to kidneys during AKI [41]. While we demonstrate SDF-1α levels were increased during AKI, they were not further increased by pFUS. AKI might maximize kidney production of SDF-1α and further elevations by pFUS were not possible. pFUS-enhanced MSC homing was likely controlled by multiple microenvironmental cues.

pFUS enhances MSC efficacy in early AKI

Previous studies have shown MSCs do not integrate into tissue, but rather act via paracrine effects to improve AKI by acting upon multiple pathophysiological pathways both locally and systemically [9, 10, 42]. MSCs located in the glomeruli and peritubular spaces can interact with tubular and immune cells through paracrine signaling, and possibly transfer of mRNA, to exert effects including stimulation of kidney regeneration, and down-regulation of inflammation and apoptosis [9, 10, 42, 43]. These infused cells can secrete factors such as VEGF, FGF, IL6, TGF-β, MCP-1, IGF-1, and SDF-1α that have been shown to improve AKI [8]. MSCs can stimulate endogenous repair/regeneration processes that are mediated by Ki67 and pAKT [44–47]. MSCs also modulate immune responses and directly suppress inflammatory macrophage, NK cell, T-cell, and B-cell function [9]. Like macrophages, which are driven toward the anti-inflammatory M2 phenotype by MSCs, MSCs can also modulate DC populations. DCs are an enormously plastic cell population and can create either pro- or anti-inflammatory microenvironments. In AKI, they have been shown among the earliest producers of many pro-inflammatory cytokines and can activate NK cells [48, 49], but are also involved in repair and regeneration in later disease stages [50]. Modulating DC populations toward an anti-inflammatory phenotype represents an important therapeutic modality in AKI [51] and MSCs have been shown to suppress DC-mediated inflammation [52, 53]. pFUS+MSCs reduced CD11c expression (a pro-inflammatory immune cell marker) on non-macrophage cells (including DCs). This may not necessarily imply a reduction in the DC population specifically, but rather a shift away from a pro-inflammatory phenotype. MSC also reduce vascular damage and preserve microcirculation by protecting endothelial cells [54].

Late therapy rescues AKI

Other MSC studies evaluated effectiveness when given early in the course of AKI. In the cisplatin model, renal function on day 1 is still within normal limits (Supplemental Figure 2) [31], and all previous studies administered MSC therapy around this time. Infusion of MSCs on D1 may simply protect against tubular damage rather than restore diminished function. It would be useful to prevent AKI when injury is foreseeable (i.e., from chemotherapy or surgically-induced ischemia), but the low incidence means that many at-risk patients would require pre-treatment with cellular therapy to prevent relatively few cases of AKI. Many clinical AKI cases (from sepsis, trauma, or inadvertent toxicity) require treatment after renal functional deficits were evident. Rescue therapy during established AKI has not been widely investigated and it has been unclear whether it is possible [55]. We performed additional studies where mice with established AKI were treated with either pFUS+MSCs or MSCs alone at D3, after renal function declined [31]. MSCs alone significantly improved 7-day survival, without functional improvements on D4 or D6. Slightly worse BUN and SCr levels were observed in mice receiving MSC alone compared to the untreated AKI cohort, but this was difficult to interpret because of data censoring (especially at D6), where function could only be measured in surviving mice. In contrast, coupling pFUS with MSC during established cisplatin-induced AKI led to statistically significant additional improvements in survival and lower BUN levels compared to MSC alone, with a trend of lower SCr levels also observed in these animals. The bias introduced by the low survival rate of untreated

AKI animals in this model prohibits more in-depth functional, histological, and molecular analyses.

Potential therapeutic mechanisms of pFUS and MSC in AKI

The improved effect of pFUS and MSC on cisplatin-induced AKI is likely in part, due to augmented MSC homing. The effects of pFUS alone remain unclear. Previous work showed unfocused ultrasound prior to ischemic/reperfusion injury improved AKI in mice [56], but its efficacy after injury was not investigated and sonication of multiple organ systems is likely when using unfocused ultrasound. pFUS to the kidney alone did not alter AKI outcomes, but did significantly alter the kidney microenvironment to enable enhanced MSC homing. MSC can secrete factors to reduce inflammation and stimulate endogenous regeneration mechanisms that are beneficial in AKI [9, 10]. Some studies suggest that MSC residing in distant organs (e.g., the lung or spleen) following i.v. infusion produce systemic changes or paracrine effects that are beneficial in AKI such that homing of MSC to injured kidney would be unnecessary [8]. However, other studies have shown that direct infusions of MSC into the renal artery will also improve AKI [57–59].

Many of our findings correlate with enhanced homing of MSC to the kidney. Using xeno-transplantation of human MSC into mice provides a unique opportunity to distinguish the source of molecular expression (i.e., MSCs or host tissue). In an effort to understand whether MSCs are acting from within the kidney or from distant organs, we surveyed human cytokine/growth factor levels in the kidney and serum. Previous studies showed that IL-10 produced by MSCs improves AKI [42]. We show that more IL-10 from human MSCs was present in the kidney after enhanced homing with pFUS+MSCs compared to MSCs alone, suggesting that enhanced MSC homing to kidneys plays a role in improved outcomes. Of the human factors surveyed in the blood and kidney tissue, only human IL-10 in the kidney was significantly increased. However, many human factors were not detected by our assay as we injected only 10^6 human MSC. While 10^6 MSC is near the limit of cells a mouse can tolerate by i.v. injection, it represents a small number of cells compared to the number of mouse cells. Thus, more sensitive methods may be necessary to detect factors produced by MSC and determine whether they are produced from within the kidney or other organs. MSC with pFUS also increased production of endogenous VEGF and reduced levels of TNFα in the kidney. TNFα has been shown to be a major driver of cisplatin-induced AKI [60] and as the disease involves severe vascular injury, modulating these factors in the kidney may be essential to improving AKI outcomes. Particularly VEGF, which was only increased in the kidney by pFUS and MSCs, correlated to increased CD31 expression. Changes in mouse VEGF and TNFα in the kidney were observed with pFUS and MSC, but these are changes in endogenous cytokines and it remains unclear whether pFUS+MSC therapy is acting on the mouse kidney or from the local microenvironment or a distant organ. Greater VEGF was also observed in the serum, but at much lower concentrations than the kidney. The tissue origin of the serum VEGF also remains unclear and the trophic factor could have been produced in the kidney before entering the circulation. MSCs alone reduced the number of NK cells in the kidney, but enhanced homing of MSC through pFUS correlated with even greater reductions and only pFUS coupled with MSC significantly reduced the number of DC. Increased tubular regeneration (Ki67 and pAKT expression) was

also seen only after MSC coupled to pFUS. MSCs shifting macrophages toward the M2 phenotype has been previously demonstrated *in vitro* [61]. While this change is observed using either MSCs alone or pFUS+MSCs, it may still be an important contributor to the enhanced effects observed with pFUS+MSCs.

It is likely that improved disease outcomes observed with pFUS and MSC were not the result of a singular signaling pathway or cellular event, but the effect of a global shift in the kidney that involves many mediators from the molecular level to cell/tissue level. While simply increasing the number of MSCs in the kidney with pFUS could amplify the therapeutic effects of MSCs, another consideration would be that pFUS-induced changes to the kidney microenvironment alter MSC function after homing occurs. pFUS could essentially precondition the kidney to both enhance MSC homing and then stimulate different cell signaling pathways compared to MSCs that home to untreated kidneys. Several studies have found that treating MSCs with various factors *in vitro* (prior to infusion) enhances their therapeutic capabilities *in vivo*. For example, pretreating MSCs with INFγ resulted in both increased production of IL-10 and reduced levels of TNFα in a mouse model of inflammatory bowel disease [62]. Another study pretreated MSCs with INFγ and either TNFα, IL-1α, or IL-1β and found all three combination pretreatments improved outcomes in mouse models of graft-versus-host disease and delayed-type hypersensitivity [63]. The pretreatment with INFγ and either TNFα, IL-1α, or IL-1β upregulated inducible nitric oxide synthase and suppressed T-cell migration to tissues where MSCs had homed. In our study, we show that pFUS pretreatment upregulates INFγ, IL-1α, and IL-1β at the early treatment time point and pFUS upregulates INFγ and IL-1α at the late therapy time point (Figure 2C). After pFUS and MSC therapy, we observed both greater MSC production of IL-10 and lower levels of TNFα in the kidney. pFUS-induced changes to the kidney microenvironment may act on MSCs, in a manner similar to the *in vitro* pretreatments of previous studies, to increase the therapeutic capacity of MSCs that home to the kidney.

Implications

This is the first demonstration that pFUS without microbubble contrast agents enhanced MSC homing to improve functional outcomes and survival in any disease model. pFUS may have clinical potential to improve cell therapies in other diseases because it allows spatio-temporal control over homing of unmodified stem cells. A critically important feature is that pFUS-enhanced homing can be readily translatable to clinical settings. Clinical pFUS instrumentation is available with sophisticated image guidance (MRI, computed tomography, or US) and can target deep structures. Moreover, the magnitude of MSC homing to pFUS-targeted tissue can be fine-tuned; it can be increased by repeated sonications coupled with repeated cell injections [23]. The spatial and temporal control over homing allows development of more sophisticated cellular treatment regimens. Currently, stem cell products are typically given to patients as a single dose and only during short windows of acute pathological inflammation (1–3 days) [64]. Acute inflammation provides necessary endogenous homing cues, but the trophic factors can subside quickly [65]. This creates two issues for cellular therapies: 1) therapy may only be beneficial when given during the acute inflammatory period, and 2) delayed or additional doses outside this window are usually less effective. Increased survival, improved renal function, and

increased levels of chemoattractants by pFUS during early AKI or clinically established AKI suggest that therapies using pFUS and MSC may be possible during subacute or chronic phases of pathology. pFUS induction of a transient “molecular zip-code” might allow multiple courses of cell therapy, a regenerative medicine approach with some promise [66], that is analogous to metronomic anti-cancer therapy. Extending the oncological analogy, pFUS can be further characterized as a neoadjuvant approach for infused cell therapies by altering the targeted microenvironment to induce an EHPR effect and improve functional outcomes. In this study, the combination of pFUS and MSC infusions was more effective than cells alone at preventing AKI and rescuing advanced AKI. Neoadjuvant pFUS with MSCs yielded the greatest improvement in organ function and survival, both of which are definitive goals for cellular therapy.

AKI is a common and consequential condition where therapeutic advances are desperately needed [1, 4, 41]. Enhanced stem cell homing with pFUS allows safe and effective AKI rescue therapy to an extent not previously observed. The ability to spatio-temporally control MSC homing precisely and noninvasively using technology approved by the FDA (albeit not yet an approved for this indication) should enable rapid translation that could improve several therapeutic strategies where cell tropism remains problematic. pFUS might also be readily implemented to enhance cell therapies for other diseases.

Supplementary Material

Refer to Web version on PubMed Central for supplementary material.

Acknowledgments

Support: This research was funded by the Intramural Research Programs of the NIH Clinical Center, the National Institute of Biomedical Imaging and Bioengineering, and the National Institute of Diabetes and Digestive and Kidney Diseases.

The authors express thanks to Dr. Ana Souza, M.D., Ph.D. (NIDDK) for helpful comments during manuscript writing.

References

1. Chertow GM, Soroko SH, Paganini EP, et al. Mortality after acute renal failure: models for prognostic stratification and risk adjustment. Kidney Int. 2006; 70:1120–1126. [PubMed: 16850028]
2. Li PK, Burdmann EA, Mehta RL. Acute kidney injury: Acute kidney injury--global health alert. Nat Rev Nephrol. 2013; 9:133–135. [PubMed: 23399583]
3. Liangos O, Wald R, O’Bell JW, et al. Epidemiology and outcomes of acute renal failure in hospitalized patients: a national survey. Clin J Am Soc Nephrol. 2006; 1:43–51. [PubMed: 17699189]
4. Star RA. Treatment of acute renal failure. Kidney Int. 1998; 54:1817–1831. [PubMed: 9853246]
5. Allgren RL, Marbury TC, Rahman SN, et al. Anaritide in acute tubular necrosis. Auriculin Anaritide Acute Renal Failure Study Group. N Engl J Med. 1997; 336:828–834. [PubMed: 9062091]
6. Hirschberg R, Kopple J, Lipsett P, et al. Multicenter clinical trial of recombinant human insulin-like growth factor I in patients with acute renal failure. Kidney Int. 1999; 55:2423–2432. [PubMed: 10354291]

7. Lewis J, Salem MM, Chertow GM, et al. Atrial natriuretic factor in oliguric acute renal failure. Anaritide Acute Renal Failure Study Group. Am J Kidney Dis. 2000; 36:767–774. [PubMed: 11007679]
8. Bi B, Schmitt R, Israilova M, et al. Stromal cells protect against acute tubular injury via an endocrine effect. J Am Soc Nephrol. 2007; 18:2486–2496. [PubMed: 17656474]
9. Togel FE, Westenfelder C. Mesenchymal stem cells: a new therapeutic tool for AKI. Nat Rev Nephrol. 2010; 6:179–183. [PubMed: 20186233]
10. Wise AF, Ricardo SD. Mesenchymal stem cells in kidney inflammation and repair. Nephrology (Carlton). 2012; 17:1–10. [PubMed: 21777348]
11. Caplan AI, Correa D. The MSC: an injury drugstore. Cell Stem Cell. 2011; 9:11–15. [PubMed: 21726829]
12. Schrepfer S, Deuse T, Reichenspurner H, et al. Stem cell transplantation: the lung barrier. Transplant Proc. 2007; 39:573–576. [PubMed: 17362785]
13. Moghadasali R, Azarnia M, Hajinasrollah M, et al. Intra-renal arterial injection of autologous bone marrow mesenchymal stromal cells ameliorates cisplatin-induced acute kidney injury in a rhesus Macaque mulatta monkey model. Cytotherapy. 2014; 16:734–749. [PubMed: 24801377]
14. Ittrich H, Lange C, Togel F, et al. In vivo magnetic resonance imaging of iron oxide-labeled, arterially-injected mesenchymal stem cells in kidneys of rats with acute ischemic kidney injury: detection and monitoring at 3T. J Magn Reson Imaging. 2007; 25:1179–1191. [PubMed: 17520738]
15. Karp JM, Leng Teo GS. Mesenchymal stem cell homing: the devil is in the details. Cell Stem Cell. 2009; 4:206–216. [PubMed: 19265660]
16. Yagi H, Soto-Gutierrez A, Parekkadan B, et al. Mesenchymal stem cells: Mechanisms of immunomodulation and homing. Cell Transplant. 2010; 19:667–679. [PubMed: 20525442]
17. Harting MT, Jimenez F, Xue H, et al. Intravenous mesenchymal stem cell therapy for traumatic brain injury. J Neurosurg. 2009; 110:1189–1197. [PubMed: 19301973]
18. Kang SK, Shin IS, Ko MS, et al. Journey of mesenchymal stem cells for homing: strategies to enhance efficacy and safety of stem cell therapy. Stem Cells Int. 2012; 2012:342968. [PubMed: 22754575]
19. Tempany CM, McDannold NJ, Hynynen K, et al. Focused ultrasound surgery in oncology: overview and principles. Radiology. 2011; 259:39–56. [PubMed: 21436096]
20. Hancock HA, Smith LH, Cuesta J, et al. Investigations into pulsed high-intensity focused ultrasound-enhanced delivery: preliminary evidence for a novel mechanism. Ultrasound Med Biol. 2009; 35:1722–1736. [PubMed: 19616368]
21. Ziadloo A, Burks SR, Gold EM, et al. Enhanced homing permeability and retention of bone marrow stromal cells by noninvasive pulsed focused ultrasound. Stem Cells. 2012; 30:1216–1227. [PubMed: 22593018]
22. Burks SR, Ziadloo A, Hancock HA, et al. Investigation of cellular and molecular responses to pulsed focused ultrasound in a mouse model. PLoS One. 2011; 6:e24730. [PubMed: 21931834]
23. Burks SR, Ziadloo A, Nguyuen BA, et al. Noninvasive pulsed focused ultrasound allows spatiotemporal control of targeted homing for multiple stem cell types in murine skeletal muscle and the magnitude of cell homing can increased through repeated applications. Stem Cells. 2013
24. Goldstein RS, Mayor GH. Minireview. The nephrotoxicity of cisplatin. Life Sci. 1983; 32:685–690. [PubMed: 6338333]
25. Yuan L, Wu MJ, Sun HY, et al. VEGF-modified human embryonic mesenchymal stem cell implantation enhances protection against cisplatin-induced acute kidney injury. Am J Physiol Renal Physiol. 2011; 300:F207–218. [PubMed: 20943766]
26. Imai N, Kaur T, Rosenberg ME, et al. Cellular therapy of kidney diseases. Semin Dial. 2009; 22:629–635. [PubMed: 20017833]
27. Zhu XY, Lerman A, Lerman LO. Concise Review: Mesenchymal Stem Cell Treatment for Ischemic Kidney Disease. Stem Cells. 2013
28. Yuen PS, Dunn SR, Miyaji T, et al. A simplified method for HPLC determination of creatinine in mouse serum. Am J Physiol Renal Physiol. 2004; 286:F1116–1119. [PubMed: 14970000]

29. Pelte CH, Chawla LS. Novel therapeutic targets for prevention and therapy of sepsis associated acute kidney injury. Curr Drug Targets. 2009; 10:1205–1211. [PubMed: 19715536]
30. Yalavarthy R, Edelstein CL. Therapeutic and predictive targets of AKI. Clin Nephrol. 2008; 70:453–463. [PubMed: 19049701]
31. Morigi M, Introna M, Imberti B, et al. Human bone marrow mesenchymal stem cells accelerate recovery of acute renal injury and prolong survival in mice. Stem Cells. 2008; 26:2075–2082. [PubMed: 18499895]
32. Fischer UM, Harting MT, Jimenez F, et al. Pulmonary passage is a major obstacle for intravenous stem cell delivery: the pulmonary first-pass effect. Stem Cells Dev. 2009; 18:683–692. [PubMed: 19099374]
33. Gheisari Y, Azadmanesh K, Ahmadbeigi N, et al. Genetic modification of mesenchymal stem cells to overexpress CXCR4 and CXCR7 does not improve the homing and therapeutic potentials of these cells in experimental acute kidney injury. Stem Cells Dev. 2012; 21:2969–2980. [PubMed: 22563951]
34. Sarkar D, Spencer JA, Phillips JA, et al. Engineered cell homing. Blood. 2011; 118:e184–191. [PubMed: 22034631]
35. Alkins R, Burgess A, Ganguly M, et al. Focused ultrasound delivers targeted immune cells to metastatic brain tumors. Cancer Res. 2013; 73:1892–1899. [PubMed: 23302230]
36. Burgess A, Ayala-Grosso CA, Ganguly M, et al. Targeted delivery of neural stem cells to the brain using MRI-guided focused ultrasound to disrupt the blood-brain barrier. PLoS One. 2011; 6:e27877. [PubMed: 22114718]
37. Ghanem A, Steingen C, Brenig F, et al. Focused ultrasound-induced stimulation of microbubbles augments site-targeted engraftment of mesenchymal stem cells after acute myocardial infarction. J Mol Cell Cardiol. 2009; 47:411–418. [PubMed: 19540842]
38. Tang HL, Wang ZG, Li Q, et al. Targeted delivery of bone mesenchymal stem cells by ultrasound destruction of microbubbles promotes kidney recovery in acute kidney injury. Ultrasound Med Biol. 2012; 38:661–669. [PubMed: 22390991]
39. Zen K, Okigaki M, Hosokawa Y, et al. Myocardium-targeted delivery of endothelial progenitor cells by ultrasound-mediated microbubble destruction improves cardiac function via an angiogenic response. J Mol Cell Cardiol. 2006; 40:799–809. [PubMed: 16678200]
40. Zhong S, Shu S, Wang Z, et al. Enhanced homing of mesenchymal stem cells to the ischemic myocardium by ultrasound-targeted microbubble destruction. Ultrasonics. 2012; 52:281–286. [PubMed: 21937069]
41. Cantaluppi V, Biancone L, Quercia A, et al. Rationale of mesenchymal stem cell therapy in kidney injury. Am J Kidney Dis. 2013; 61:300–309. [PubMed: 22938846]
42. Milwid JM, Ichimura T, Li M, et al. Secreted factors from bone marrow stromal cells upregulate IL-10 and reverse acute kidney injury. Stem Cells Int. 2012; 2012:392050. [PubMed: 23319959]
43. Nemeth K, Leelahavanichkul A, Yuen PS, et al. Bone marrow stromal cells attenuate sepsis via prostaglandin E(2)-dependent reprogramming of host macrophages to increase their interleukin-10 production. Nat Med. 2009; 15:42–49. [PubMed: 19098906]
44. Imberti B, Morigi M, Benigni A. Potential of mesenchymal stem cells in the repair of tubular injury. Kidney international supplements. 2011; 1:90–93. [PubMed: 25028629]
45. Nguan CY, Guan Q, Gleave ME, et al. Promotion of cell proliferation by clusterin in the renal tissue repair phase after ischemia-reperfusion injury. Am J Physiol Renal Physiol. 2014; 306:F724–733. [PubMed: 24477687]
46. Rota C, Imberti B, Pozzobon M, et al. Human amniotic fluid stem cell preconditioning improves their regenerative potential. Stem Cells Dev. 2012; 21:1911–1923. [PubMed: 22066606]
47. Ye Y, Wang B, Jiang X, et al. Proliferative capacity of stem/progenitor-like cells in the kidney may associate with the outcome of patients with acute tubular necrosis. Human pathology. 2011; 42:1132–1141. [PubMed: 21315412]
48. Dong X, Swaminathan S, Bachman LA, et al. Resident dendritic cells are the predominant TNF-secreting cell in early renal ischemia-reperfusion injury. Kidney Int. 2007; 71:619–628. [PubMed: 17311071]

49. Okusa MD, Li L. Dendritic cells in acute kidney injury: cues from the microenvironment. Transactions of the American Clinical and Climatological Association. 2012; 123:54–62. discussion 62–53. [PubMed: 23303968]
50. Molitoris BA. Therapeutic translation in acute kidney injury: the epithelial/endothelial axis. J Clin Invest. 2014; 124:2355–2363. [PubMed: 24892710]
51. Li L, Huang L, Ye H, et al. Dendritic cells tolerized with adenosine A(2)AR agonist attenuate acute kidney injury. J Clin Invest. 2012; 122:3931–3942. [PubMed: 23093781]
52. Ma S, Xie N, Li W, et al. Immunobiology of mesenchymal stem cells. Cell death and differentiation. 2014; 21:216–225. [PubMed: 24185619]
53. Singh-Jasuja H, Thiolat A, Ribon M, et al. The mouse dendritic cell marker CD11c is down-regulated upon cell activation through Toll-like receptor triggering. Immunobiology. 2013; 218:28–39. [PubMed: 22445076]
54. Togel F, Weiss K, Yang Y, et al. Vasculotropic, paracrine actions of infused mesenchymal stem cells are important to the recovery from acute kidney injury. Am J Physiol Renal Physiol. 2007; 292:F1626–1635. [PubMed: 17213465]
55. Okusa MD, Molitoris BA, Palevsky PM, et al. Design of clinical trials in acute kidney injury: a report from an NIDDK workshop--prevention trials. Clin J Am Soc Nephrol. 2012; 7:851–855. [PubMed: 22442188]
56. Gigliotti JC, Huang L, Ye H, et al. Ultrasound prevents renal ischemia-reperfusion injury by stimulating the splenic cholinergic anti-inflammatory pathway. J Am Soc Nephrol. 2013; 24:1451–1460. [PubMed: 23907510]
57. Togel F, Weiss K, Yang Y, et al. Vasculotropic, paracrine actions of infused mesenchymal stem cells are important to the recovery from acute kidney injury. Am J Physiol Renal Physiol. 2007; 292:F1626–1635. [PubMed: 17213465]
58. Zhuo W, Liao L, Fu Y, et al. Efficiency of endovenous versus arterial administration of mesenchymal stem cells for ischemia-reperfusion-induced renal dysfunction in rats. Transplant Proc. 2013; 45:503–510. [PubMed: 23498785]
59. Behr L, Hekmati M, Fromont G, et al. Intra renal arterial injection of autologous mesenchymal stem cells in an ovine model in the postischemic kidney. Nephron Physiology. 2007; 107:65–76.
60. Ramesh G, Reeves WB. TNF-alpha mediates chemokine and cytokine expression and renal injury in cisplatin nephrotoxicity. J Clin Invest. 2002; 110:835–842. [PubMed: 12235115]
61. Wise AF, Williams TM, Kiewiet MB, et al. Human mesenchymal stem cells alter macrophage phenotype and promote regeneration via homing to the kidney following ischemia/reperfusion injury. Am J Physiol Renal Physiol. 2014
62. Duijvestein M, Wildenberg ME, Welling MM, et al. Pretreatment with interferon-gamma enhances the therapeutic activity of mesenchymal stromal cells in animal models of colitis. Stem Cells. 2011; 29:1549–1558. [PubMed: 21898680]
63. Kavanagh DP, Robinson J, Kalia N. Mesenchymal stem cell priming: fine-tuning adhesion and function. Stem Cell Rev. 2014; 10:587–599. [PubMed: 24752328]
64. Huang J, Zhang Z, Guo J, et al. Genetic modification of mesenchymal stem cells overexpressing CCR1 increases cell viability, migration, engraftment, and capillary density in the injured myocardium. Circ Res. 2010; 106:1753–1762. [PubMed: 20378860]
65. Komatsu K, Honmou O, Suzuki J, et al. Therapeutic time window of mesenchymal stem cells derived from bone marrow after cerebral ischemia. Brain Res. 2010; 1334:84–92. [PubMed: 20382136]
66. Zhang L, Li K, Liu X, et al. Repeated systemic administration of human adipose-derived stem cells attenuates overt diabetic nephropathy in rats. Stem Cells Dev. 2013; 22:3074–3086. [PubMed: 23844841]

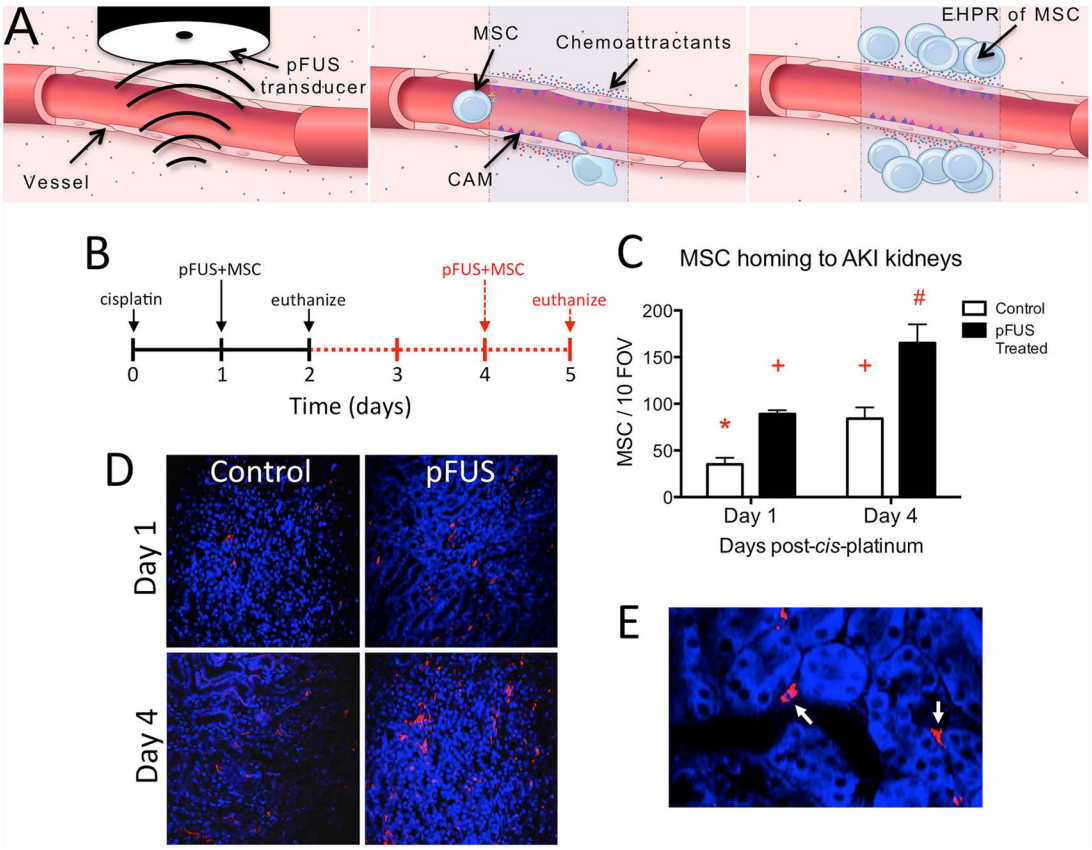

Figure 1. Schematic of enhanced homing permeability and retention (EHPR) of MSC by pFUS and pFUS-induced EHPR of MSC during AKI

A) pFUS interacts with the parenchyma, interstitium and vasculature (*Left panel*). Levels of vascular integrins (ICAM and VCAM) and chemoattractants (soluble cytokines, chemokines, and trophic factors) increase in the treated volume (*Center panel*). Intravascularly injected stem cells (e.g. MSC) tether to cell adhesion molecules expressed on endothelial cell surfaces and extravasate in response to gradients of chemoattractants (*Right panel*). Schematic not shown to scale. B**) Experimental timeline showing treatment schedules for two cohorts of mice**. All mice received cisplatin on D0 (n=5 mice/group). On either D1 (black solid lines) or D4 (red dashed lines), mice received unilateral pFUS followed by i.v. human MSCs 4h later. Mice were euthanized 24h post-injection and MSC homing to pFUS-treated and untreated contralateral kidneys was quantified by immunofluorescence for human mitochondria. **C) pFUS induced significantly greater MSC homing to kidneys on either D1 or D4.** MSC homing to pFUS-treated kidneys was ~2-fold greater on either day compared to untreated kidneys on the same day. Significantly greater MSC homing was observed to contralateral kidneys on D4 compared to D1, possibly reflecting greater levels of signaling molecules shown in Fig 3A. Homing for all groups was compared by ANOVA ($p<0.05$) where like symbols indicate statistical similarity and different symbols indicate statistical differences (FOV; field of view). **D) Representative human mitochondrial staining.** Immunofluorescence imaging (10×) shows human MSCs

in pFUS and control kidneys **E) A high-magnification view of human mitochondrial staining (100×).** MSCs are localized to peri-tubular spaces.

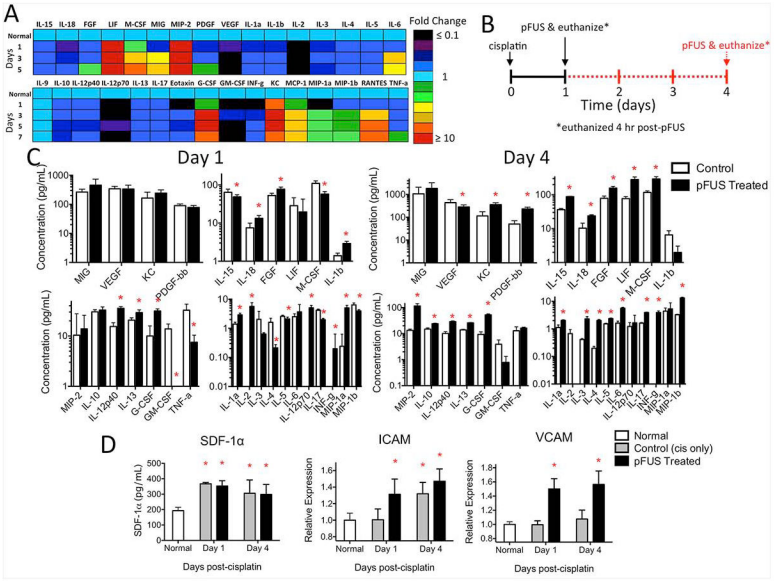

Figure 2. Kidney profile of cytokines, chemokines, growth factors, and integrins in kidneys during AKI with and without pFUS

A) Heat map showing fold changes in kidney signaling molecules over time during AKI (no pFUS, no MSC). Days indicated are time points post-cisplatin and "normal" represents saline-treated animals (no cisplatin). Few increases are detected at D1 and trends of sub-physiological expression for many factors are observed. Trends of increased expression of many factors are evident by D3 and persist until D5 (n=6 mice/group). **B) Experimental timeline for C and D showing two cohorts of mice that received cisplatin on D0 and then pFUS either on D1 (black solid line) or D4 (red dashed line). C) pFUS-induced changes in kidney signaling molecules following unilateral pFUS on D1 or D4 (no MSC).** Mice from both days were euthanized 4h post-pFUS (n=6 mice/group). Tissue levels in pFUS-treated kidneys were analyzed by multiplex ELISA and compared to untreated contralateral kidneys on the same day by *t*-tests (* $p<0.05$). Significant changes in molecular expression were evident following pFUS on either day—most factors increased following pFUS, but decreases were also observed for some. **D) Changes in SDF-1α, ICAM, and VCAM expression during AKI and effects of pFUS.** pFUS-treated and contralateral control AKI kidneys (no pFUS) from the indicated day, in addition to normal kidneys (n=6 mice/group), were analyzed by single-plex ELISA. Data for each group were compared to all other groups by ANOVA (* $p<0.05$). Control AKI kidneys (no pFUS) showed elevations in SDF-1α above normal kidneys at D1 and D4, but no additional increases were observed following pFUS of AKI kidneys. ICAM in control AKI kidneys was not elevated compared to normal kidneys on D1, but pFUS induced greater D1 ICAM expression. ICAM in control AKI kidneys was significantly greater than normal kidneys on D4, but pFUS failed to induce further increases. VCAM was not increased in control AKI kidneys at either day compared to normal kidneys, but pFUS at either day increased VCAM in AKI kidneys.

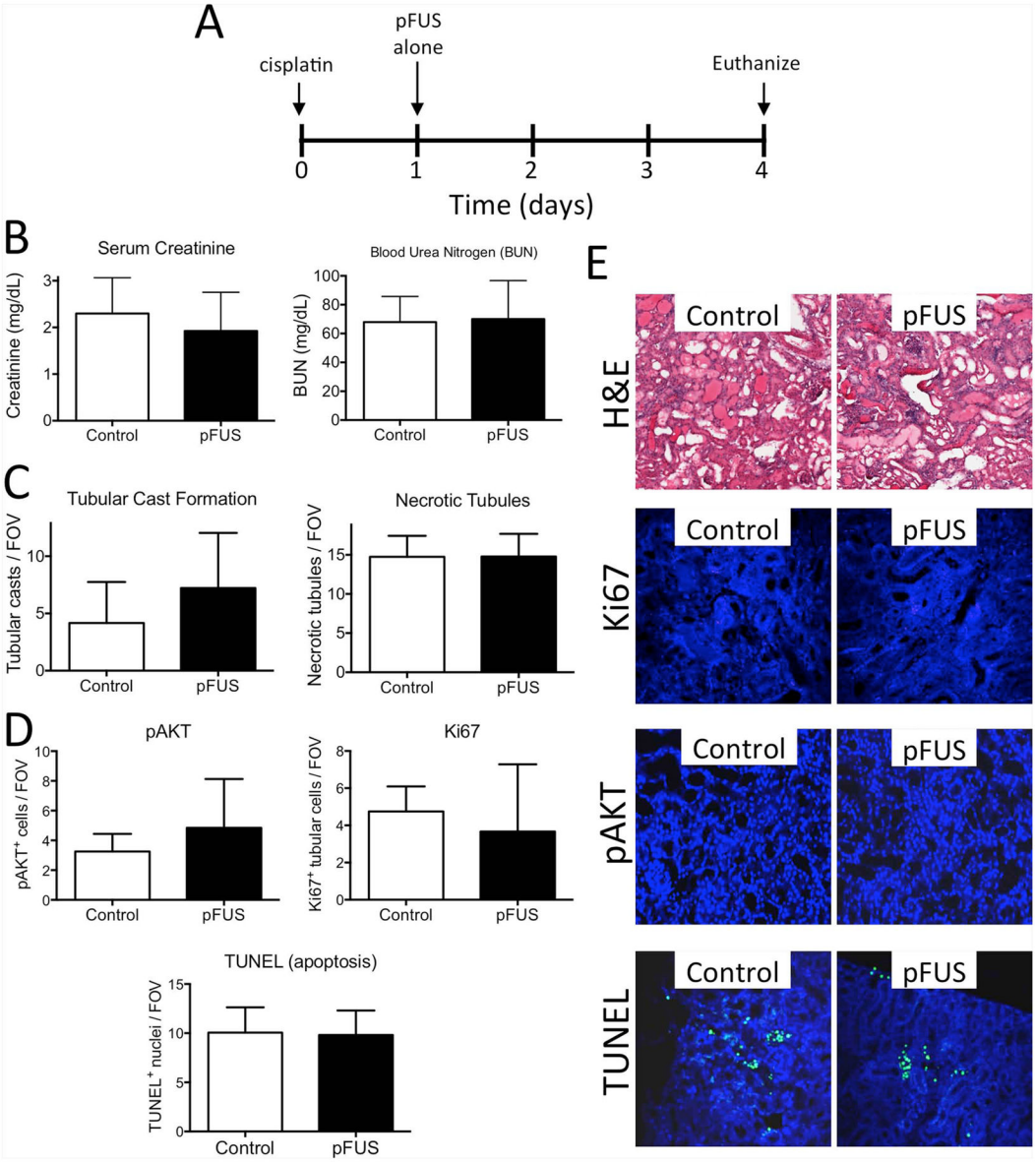

Figure 3. pFUS alone (no MSCs) does not alter AKI outcomes

A) Experimental timeline. Mice were given cisplatin on D0 and then either bilateral pFUS or sham pFUS (transducer power=0 W) on D1 (n=6 mice per group). Mice were euthanized on D4 and AKI was assessed by **B)** BUN and SCr levels, **C)** histological features such as necrotic tubules and tubular casts, and **D)** apoptosis (TUNEL) regeneration (pAKT), and proliferation (Ki67). These were unchanged by pFUS alone. **E)** Representative images for renal histology, TUNEL and Ki67 staining. Measurements between pFUS-treated and control kidneys were compared by *t*-tests and found not to be significant ($p>0.05$).

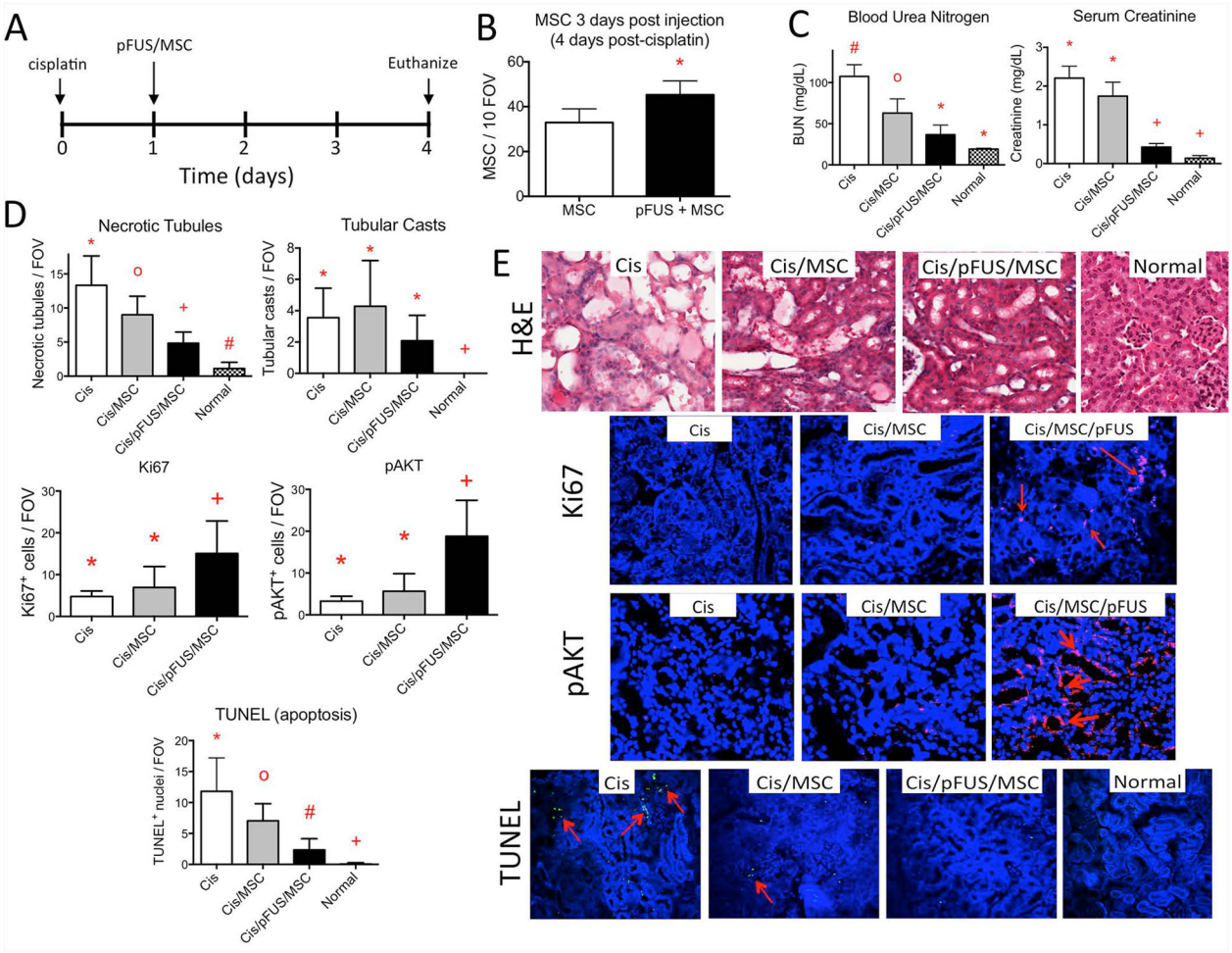

Figure 4. Coupling pFUS and MSC during early AKI leads to less severe disease

A) Experimental timeline. Normal mice, control AKI mice, and AKI mice treated with pFUS and/or MSC received appropriate treatment on D1 and were euthanized for analyses on D4. **B)** MSC with pFUS on D1 leads to better MSC retention in pFUS-treated kidneys at D4 compared to kidneys that received MSC alone (* $p<0.05$ following *t*-test). **C) Coupling pFUS with MSC (Cis/pFUS/MSC) on D1 leads to better renal function at D4.** BUN is significantly decreased by MSC alone and further decreased by pFUS with MSC. SCr is not improved by MSC alone, but is improved by pFUS+MSC. Groups with like symbols are statistically similar to each other and statistically different from groups with different symbols after ANOVA ($p<0.05$) (n=5–7 mice/group). **D and E) Molecular and histological profiles of kidneys on D4 after pFUS and/or MSC on D1.** Statistical summaries are shown in D, while representative microscopic images are shown in E. By H&E, the number of necrotic tubules was significantly decreased following MSC alone and further significantly decreased by pFUS+MSC, however no improvement in tubular cast number was observed for either group. pAKT and Ki67 expression were significantly increased only after pFUS with MSC. The number of apoptotic cells (red arrows) was reduced by MSC alone and further reduced by pFUS and MSC. Groups with like symbols

are statistically similar to each other and statistically different from groups with different symbols after ANOVA ($p<0.05$) (n=5–7 mice/group).

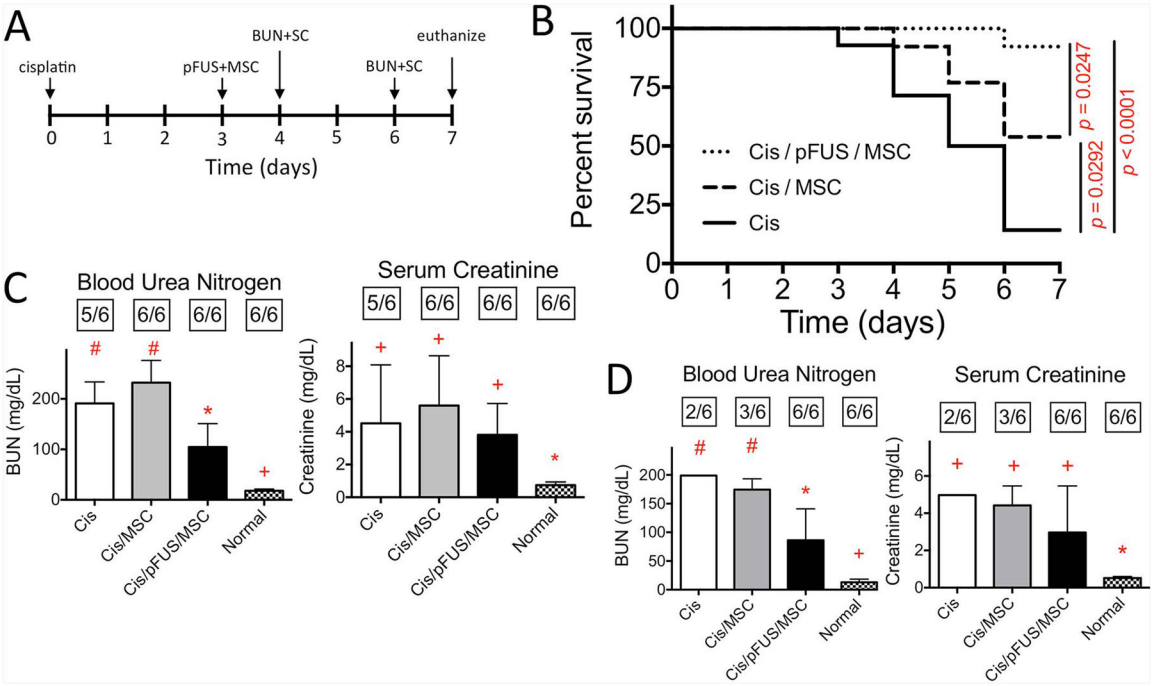

Figure 5. Treating AKI with MSC alone after functional deficits manifest improves survival and coupling pFUS and MSC further improves survival and renal function

A) Experimental timeline. pFUS and/or MSC treatment was administered at D3 with renal functional measurements at D4 and D6. **B) Kaplan-Meier curves of survival following treatment at D3**. Survival is significantly increased following MSC alone (Cis/MSC) compared to untreated mice (Cis) (p=0.0292), while pFUS+MSC (Cis/pFUS/MSC) yields better survival compared to MSC alone (p=0.0247) or untreated mice (p<0.0001) using log-rank tests (n=14 mice/group). **C) Renal function (BUN and SCr) measurements at D4 (24h post-treatment).** BUN significantly improved after pFUS with MSC. The number of mice surviving to the measurement time point is indicated in boxes above each bar. Groups with like symbols are statistically similar to each other and statistically different from groups with different symbols after ANOVA (p<0.05). **D) Renal function (BUN and SCr) measurements at D6 (72h post-treatment)**. Significant improvements in BUN clearance persist to D6 only after pFUS+MSC. The number of mice surviving to the measurement time point is indicated above each bar. Variance of the “Cis” group in panel D is omitted because n=2. Groups with like symbols are statistically similar to each other and statistically different from groups with different symbols after ANOVA (p<0.05).

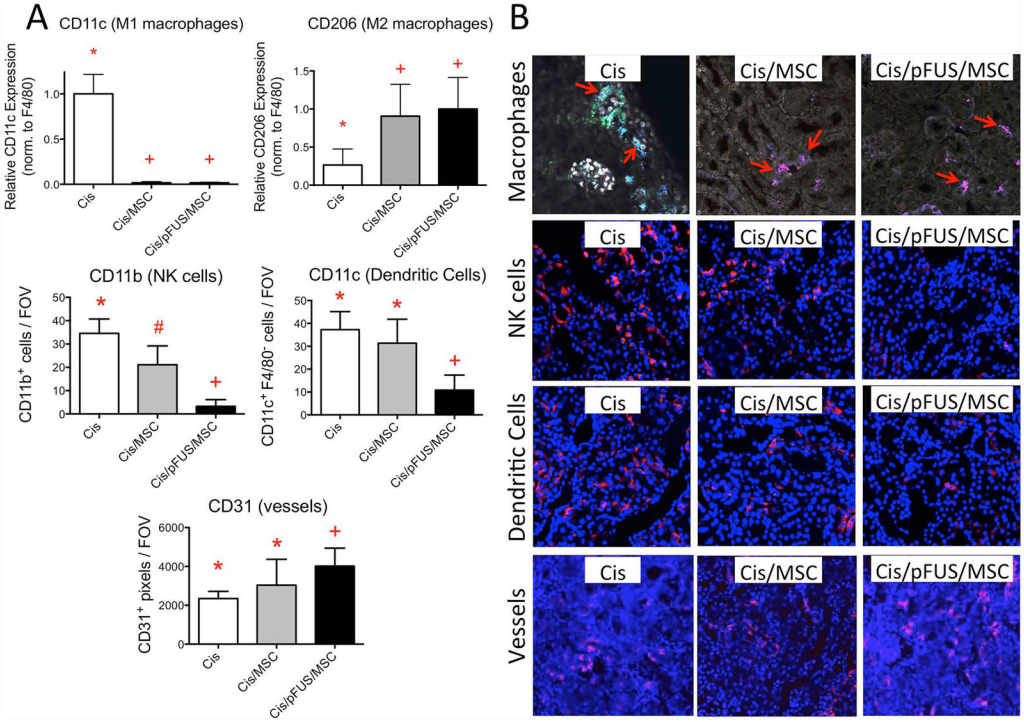

Figure 6. Effects of MSCs with or without pFUS on immune cell populations and blood vessel density

The experimental timeline was Cisplatin on D0, pFUS and/or MSC on D1, euthanasia on D2. **A)** Statistical summaries of immune cell populations and blood vessels following treatment. CD11c and CD206 expression F4/80-positive cells. Macrophages appear more M2-like after MSC alone or pFUS+MSC (*top row*). CD11b expressed by natural killer (NK) cells and is reduced by MSC alone and further reduced by pFUS+MSC. Non-macrophage CD11c (e.g., on dendritic cells [DC]) is unchanged by MSC alone, but reduced following pFUS+MSC (*middle row*). CD31 expressed by endothelial cells is not significantly increased by MSC alone, but is significantly increased by pFUS+MSC (*bottom row*). Groups with like symbols are statistically similar to each other and statistically different from groups with different symbols after ANOVA ($p<0.05$) (n=4 mice per group) **B)** Representative IHC staining of AKI kidneys. The top row shows F4/80 (all macrophages; blue), CD11c (M1 macrophages; green), and CD206 (M2 macrophages; red) staining. The second row shows CD11b (red) expressed on natural killer (NK) cells. The third row shows non-macrophage CD11c (red) expressed by dendritic cells (DC) and the fourth row shows CD31 (red) expressed by endothelial cells.

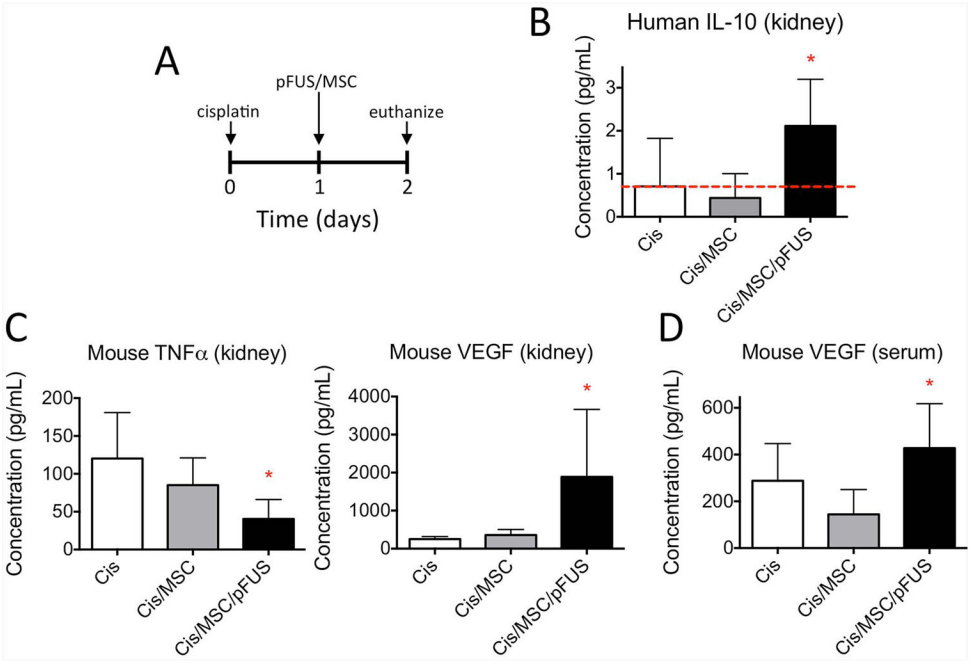

Figure 7. Changes in human and mouse cytokines in the kidney and serum following MSC treatment or combination MSC and pFUS treatment

A) Experimental timeline showing treatment and euthanasia (n=6 mice per group). **B)** Greater human IL-10 produced by human MSC is present in the kidney following pFUS +MSC. Red line indicates assay signal from control AKI mice (no MSCs) that corresponds to background levels of signal. **C)** Lower levels of mouse TNFa and increased levels of mouse VEGF are present in mouse kidney following pFUS+MSC. **D)** Increased mouse VEGF is observed in the serum following pFUS+MSC.